Borrelia burgdorferi engages mammalian type I interferon responses via the cGAS-STING pathway

Lauren C. Farris[1], Sylvia Torres-Odio[1], L. Garry Adams[2], A. Phillip West[1*], and Jenny A. Hyde[1*]

[1]Department of Microbial Pathogenesis and Immunology, College of Medicine, Texas A&M University, Bryan, TX, USA

[2]Department of Veterinary Pathobiology, College of Veterinary Medicine and Biomedical Sciences, Texas A&M University, College Station, TX, USA

Running Title: *Borrelia burgdorferi activates the cGAS-STING pathway*

Funding: This work was supported by NIH grant R21AI153879 to A.P.W. and J.A.H. S.T.-O. was supported by NRSA predoctoral training award F31HL160141 from NIH.

***Correspondence:** Address correspondence and reprint requests to Dr. A. Phillip West or Dr. Jenny A. Hyde, Texas A&M University College of Medicine, 8447 Riverside Parkway, Bryan, TX 77807. Email: awest@tamu.edu or jhyde@tamu.edu.

Keywords: *Borrelia burgdorferi*, Lyme disease, innate immunity, type I interferon, cGAS, STING

ABSTRACT

Borrelia burgdorferi, the etiologic agent of Lyme disease, is a spirochete that modulates numerous host pathways to cause a chronic, multi-system inflammatory disease in humans. *B. burgdorferi* infection can lead to Lyme carditis, neurologic complications, and arthritis, dependent upon the ability of specific borrelial strains to disseminate, invade, and drive inflammation. *B. burgdorferi* elicits type I interferon (IFN-I) responses in mammalian cells and tissues that are associated with the development of severe arthritis or other Lyme-related complications. However, the innate immune sensors and signaling pathways controlling IFN-I induction remain unclear. In this study, we examined whether intracellular nucleic acid sensing is required for the induction of IFN-I to *B. burgdorferi*. Using confocal microscopy, we show that *B. burgdorferi* is taken up by mouse and human cells in culture, indicating a route for intracellular detection. In addition, we report that IFN-I responses in primary mouse macrophages and murine embryonic fibroblasts are significantly attenuated in the absence of the pattern recognition receptor cyclic GMP-AMP synthase (cGAS) or its adaptor Stimulator of Interferon Genes (STING), which function together to sense and respond to intracellular DNA. In vivo tracking of bioluminescent *B. burgdorferi* during infection of C57BL/6 wild-type, cGAS knockout, or STING deficient mice revealed similar dissemination kinetics and borrelial load. However, tibiotarsal joint pathology and inflammation were reduced in cGAS knockout compared to wild-type mice. Collectively, these results indicate that the cGAS-STING pathway is an innate immune sentinel of *B. burgdorferi* that plays a key role in the induction of mammalian IFN-I responses.

INTRODUCTION

Lyme disease results from infection with the spirochetal bacterium *Borrelia burgdorferi* and presents as a multi-systemic inflammatory disease causing debilitating morbidity due to fatigue, malaise, severe arthritis, and cardiac and neurologic complications (1–4). It is the most common tick-borne disease in the United States and is a significant public health concern, with the CDC reporting 39,000 cases per year but insurance reports indicating prevalence greater than 470,000 cases per year (5–7). Antibiotic treatment is highly effective when administered shortly after the tick bite, yet antibiotic efficacy declines as the borrelial infection progresses (8, 9). Lyme disease occurs in localized, disseminated, and late stages as the extracellular pathogen hematogenously spreads from the site of the tick bite to secondary colonized tissues, including the joints, heart, and central nervous system, causing Lyme arthritis, carditis, and neuroborreliosis respectively (1–3, 8). The development of arthritis, a characteristic symptom of late Lyme disease in North America, is associated with a robust innate immune response that includes induction of type I interferon (IFN-I) cytokines (10–12).

B. burgdorferi elicits a robust innate immune response, resulting in the secretion of pro-inflammatory cytokines and chemokines (13–20). In addition, *B. burgdorferi* triggers IFN-I responses in a wide array of human cells, mouse cells, and infected tissues (11–13, 19, 21–28). Evidence suggests that innate IFN-I signaling plays key roles in several aspects of *B. burgdorferi* pathology (29–33). Notably, IFN-I and resulting interferon-stimulated gene (ISG) signatures are linked to the development of more severe arthritis in experimental models, and also correlate with lingering neurocognitive symptoms of Lyme disease (12, 30, 32, 34). In addition, a recent study from Lochhead and colleagues observed that a robust interferon gene signature correlates with decreased expression of tissue repair genes in synovial lesion biopsies from patients with

postinfectious, *B. burgdorferi*-induced Lyme arthritis (35). It is well-appreciated that innate immune sensing of the abundant *B. burgdorferi* lipoproteins via Toll-like receptor 2 (TLR2) triggers production of pro-inflammatory cytokines and chemokines in vitro and in vivo (14, 36–38). However, lipoprotein binding to TLR2 is not a robust inducer of IFN-I responses in most mouse and human cell types (39, 40). Studies using human cells have implicated nucleic acid sensing TLRs (TLR 7, 8, and 9) as regulators of IFN-I induction in human immune cells challenged with *B. burgdorferi* in vitro (13, 18, 19). In contrast, other reports have shown that *B. burgdorferi* can engage IFN-I responses in non-phagocytic fibroblasts and endothelial cells, which do not express a full complement of TLRs (25, 41). Moreover, ISG induction in murine macrophages is independent of the two primary TLR adaptor proteins MyD88 and TRIF (22, 23). Thus, TLR-mediated sensing of *B. burgdorferi* pathogen-associated molecular patterns does not appear to be the predominant trigger of IFN-I responses in mammalian cells during infection.

Innate immune pathways that sense cytosolic nucleic acids, such as the RIG-I-like receptor (RLR)-Mitochondrial Antiviral Signaling (MAVS) or Cyclic GMP-AMP synthase (cGAS)-Stimulator of Interferon Genes (STING) pathway, have emerged as key regulators of IFN-I production in both immune and non-immune cells (42–49). Cyclic GMP-AMP synthase (cGAS) is an intracellular DNA sensor that localizes to the mammalian cell cytoplasm and nucleus. Upon binding intracellular pathogen DNA, micronuclei, or mitochondrial DNA, cGAS generates the non-canonical cyclic dinucleotide, 2’3’-cyclic guanosine monophosphate-adenosine monophosphate (cGAMP), which binds STING. This results in the recruitment and activation of Tank-binding Kinase 1 (TBK1), leading to the phosphorylation of Interferon Regulatory Factor 3 (IRF3) for the induction of type I interferons (IFNα, β) and ISGs (42–44). Although initially identified as an antiviral host defense pathway, it is now well known that the cGAS-STING

pathway is critical for induction of robust IFN-I responses to intracellular bacteria such as *Mycobacterium tuberculosis* and *Listeria monocytogenes* (45, 50, 51). A recent study revealed that the cGAS-STING pathway is also essential for IFN-I production in response to multiple extracellular pathogens, including *Pseudomonas aeruginosa*, *Klebsiella pneumoniae*, and *Staphylococcus aureus* (52, 53). *B. burgdorferi*, predominantly an extracellular pathogen, is readily taken up by phagocytic cells and may also internalize into endothelial cells and fibroblasts, which are key sources of IFN-I in the Lyme disease joint (54–62). *B. burgdorferi* also produces cyclic dinucleotides c-di-GMP and c-di-AMP, which can directly engage STING (63–66). Thus, there are several potential routes by which *B. burgdorferi* infection could trigger the cGAS-STING-IFN-I pathway.

In this study, we tested the hypothesis that *B. burgdorferi* infection induces IFN-I through the cGAS-STING pathway. We exposed phagocytic and non-phagocytic cells lacking various components of the cytosolic nucleic acid sensing machinery to viable and sonicated *B. burgdorferi* and evaluated IFN-I and ISG expression after exposure. Furthermore, we performed an infectivity study with bioluminescent *B. burgdorferi* in mice deficient in cGAS or STING to assess borrelial load by in vivo imaging and joint inflammation using histopathology. Our results reveal that *B. burgdorferi* engages IFN-I responses in a cGAS-STING dependent manner that contributes to joint inflammation without significantly altering infection kinetics or borrelial load in tissues.

MATERIALS AND METHODS

Mouse and *B. burgdorferi* strains

C57BL/6J (strain 000664), cGAS KO (C57BL/6N-Cgas$^{tm1d(EUCOMM)Hmgu}$/J, strain 026554), Sting$^{gt/gt}$ (C57BL/6J-Sting1^{gt}/J, strain 017537), IFNAR$^{-/-}$ (B6(Cg)-Ifnar1$^{tm1.2Ees/J}$, strain 028288) and MAVS$^{-/-}$ (B6;129-*Mavs*^{tm1Zjc}/J, strain 008634) were obtained from the Jackson Laboratory. MAVS-/- mice were backcrossed to C57BL/6J mice for 10 generations before generation of primary cell lines. All animal experiments were conducted in accordance with the guidelines established by the Texas A&M University Institutional Animal Care and Use Committee.

Low-passage *B. burgdorferi* strains B31-A3 and ML23 pBBE22*luc* was cultured in BSK-II medium with 6% normal rabbit serum (NRS) (Pel-Freeze Biologicals, Rogers, AR) and grown to mid-log phase at 37°C at 5% CO_2(67–71). ML23 pBBE22*luc* cultures were supplemented with 300 µg/ml kanamycin.

Cell culture and borrelial infections

Mouse embryonic fibroblasts (MEFs) were harvested from WT, cGAS$^{-/-}$, STING $^{gt/gt}$, IFNAR$^{-/-}$, and MAVS$^{-/-}$ embryos from E12.5 to 14.5. BMDMs were harvested and differentiated in media containing L929 supernatant (CCL-1, ATCC, Manassas, VA). Human foreskin fibroblasts (HFF-1, SCRC-1041, ATCC) were immortalized using a human telomerase expressing retrovirus containing pWZL-Blast-Flag-HA-hTERT (22396, Addgene, Watertown, MA). Cells were grown in DMEM (D5756-500ML; Sigma-Aldrich) with 10% FBS (VWR International). Primary cell lines were cultured for no more than four passages prior to experiments.

Bacteria were prepared as previously described (61) with the following exceptions. *B. burgdorferi* was grown to mid-exponential phase, centrifuged at 6600 xg for 8 minutes, washed twice in PBS, and resuspended in DMEM (D5796-500ml, Millipore Sigma) with 10% FBS (VWR). Spirochetes were enumerated using dark-field microscopy and diluted to the appropriate

MOI. Where indicated, plates were spun following the addition of bacteria to mammalian cells for 5 minutes at 300 xg.

Quantitative PCR and RT-PCR

RNA was isolated from mammalian cells using the Quick-RNA Micro Prep Kit (R1051; Zymo Research) according to the manufacturer's instructions. Between 300-500 ng of RNA was standardized across samples from each experiment and converted to cDNA with the qScript cDNA Synthesis Kit (QuantaBio, Beverly, MA). Quantitative PCR (qPCR) was performed on cDNA using the PerfecTa SYBR Green FastMix (Quantabio) and primers listed in Table I. Each biological sample was assayed in triplicate. Relative expression was determined for each replicate through normalization against a housekeeping gene (*Bactin* or *GAPDH*) using the $2^{-\Delta\Delta CT}$ method. DNA contamination of RNA samples was evaluated in a single, no RT reaction for each primer set.

Immunoblotting

Protein was collected from cells lysed in 1% NP-40 buffer and spun for 10 minutes at 17,000 xg at 4°C. The supernatant was collected and stored at -80°C. Protein lysates were quantified using the micro-BCA assay (ThermoFisher Scientific, Waltham, MA). Immunoblotting was performed as described in (72). Briefly, between 20-30 μg of protein was separated on a 10-20% polyacrylamide gel and transferred to a polyvinylidene difluoride (PVDF) membrane at 100V for 1 hour. Membranes were dried for 30 minutes and incubated with primary antibodies (Table II) overnight at 4°C. Membranes were washed in 1X PBS for 30 minutes before incubation with HRP-conjugated secondary antibodies for 1 hour. Membranes were washed again in PBS for 1

hour and developed with Millipore Luminata Crescendo HRP substrate (MilliporeSigma, Burlington, MA).

Immunofluorescence microscopy

Cells were seeded on 12- or 18-mm sterile coverslip, allowed to adhere overnight, and infected as described above. At the conclusion of infection, cells were washed with DMEM and then 1X PBS, fixed with 4% paraformaldehyde for 15 minutes at room temperature, and washed twice with 1X PBS for 5 minutes each. Cells were permeabilized with 0.1% Triton X-100 in PBS for 5 minutes at RT, washed twice with 1X PBS and blocked for 30 minutes in PBS containing 5% FBS. Each coverslip was stained with primary and secondary antibodies for 1 hour each. Cells were washed in 1X PBS with 5% FBS three times after each stain for 5 minutes each. Coverslips were mounted with ProLong Gold mounting medium containing DAPI (Molecular Probes) and allowed to dry overnight. Fluorescent images were captured on a Zeiss LSM 780 confocal microscope system with a 63X oil-immersion objective. Z-stack images were processed using Zeiss ZEN software.

Mouse infection with *B. burgdorferi* with in vivo bioluminescent imaging

Bioluminescent images of mice were collected as previously described (70, 73). Groups of 5 WT, cGAS$^{-/-}$, and STING$^{gt/gt}$ male mice 6-11 weeks old were intradermally injected with 10^5 ML23 pBBE22*luc.* Prior to imaging, 5 mg of D-luciferin (Goldbio, St. Louis, MO) was dissolved in PBS and administered to all except one mouse per group via intraperitoneal injection and anesthetized with isoflurane for imaging. Mice were imaged at 1 hour and 1, 4, 7, 10, 14, 21, and 28 days post-infection (dpi) using the Perkin Elmer IVIS Spectrum live imaging system.

Bioluminescence from treated mice were normalized to the untreated mouse from each group. At 28 dpi, inguinal lymph nodes and skin flanks were collected and transferred to BSKII with 6% NRS for outgrowth assays.

Histopathology

Samples of joints and hearts were collected from each mouse following euthanasia at 28 and 35 dpi, fixed by immersion in 10% neutral buffered formalin at room temperature for 48 hours, and stored in 70% ethanol before embedding in paraffin, sectioning at 5-6 µm, and staining with hematoxylin and eosin by AML Laboratories, Inc. (Jacksonville, Florida). The tissue sections were examined using brightfield microscopy in a blinded manner by a board-certified anatomic veterinary pathologist and ordinally scored for the degree of mononuclear infiltration. Score of 1 represented minimal infiltration (<5 cells/400X field) and increased to 4 for abundant infiltration (>30cells/400X field). Tissue sections were also scored for distribution of mononuclear inflammatory cells as focal (1), multifocal (2), or diffuse (3).

Statistical analyses

Statistical analysis was performed in GraphPad Prism (GraphPad Software, Inc., La Jolla, CA). Statistical significance was determined by $p \leq 0.05$. Specific tests are detailed in the figure legends. Error bars in figures represent standard error of the mean (SEM) based on the combined technical replicates for biological duplicates.

Animal ethics statement

Texas A&M University is accredited by the Association for Assessment and Accreditation of Laboratory Animal Care (AAALAC) indicating their commitment to responsible animal care and use. All animal experiments were performed in accordance with the Guide for Care and Use of Laboratory Animals provided by the National Institute of Health (NIH) and the Guidelines of the Approval for Animal Procedures provided by the Institutional Animal Care and Use Committee (IACUC) at Texas A&M University.

RESULTS

Viable *B. burgdorferi* elicits a robust type I interferon response in mouse macrophages and fibroblasts.

We first evaluated the ability of primary bone marrow-derived macrophages (BMDM) and embryonic fibroblasts (MEF) isolated from C57BL/6J mice to upregulate interferon stimulated genes (ISGs) and inflammatory cytokine transcripts when co-incubated with viable or sonicated *B. burgdorferi* B31-A3 at a MOI 20 for 6 or 24 hours, respectively (Fig. 1). Consistent with earlier reports (19, 60), both viable and sonicated B31-A3 were able to induce *Ifnb1* and ISGs (*Cxcl10, Gbp2*), in addition to pro-inflammatory cytokine (*Il6*) expression, in BMDMs (Fig. 1A-B). Viable *B. burgdorferi* more potently induced ISGs and *Il6* (~6-8 fold higher) than sonicated bacteria. Likewise, we found that *B. burgdorferi* elicited ISGs and *Tnfa* in MEFs, with live spirochetes triggering more robust responses compared to sonicated bacteria (Fig. 1C-D). Collectively, these data indicate that live *B. burgdorferi* engages robust IFN-I-associated ISG expression in both BMDMs and non-phagocytic MEFs, which lack a full repertoire of TLRs and other pattern recognition receptors (PRRs) (41).

B. burgdorferi engages the cGAS-STING pathway to induce IFN-I.

Lipoprotein rich *B. burgdorferi* predominately engage TLR2, but can also trigger other TLRs to induce inflammatory cytokines and interferons (18, 19, 24, 36). However, whether cytosolic DNA sensing is a component of the innate immune response to *B. burgdorferi* remains unknown. To examine this directly, we co-cultured primary BMDMs derived from wild type (WT), cGAS$^{-/-}$ or STING$^{gt/gt}$ C57BL/6J mice with *B. burgdorferi* B31-A3 for 6 and 9 hours, and preformed RNA, protein, and confocal microscopic analyses (Fig. 2). Notably, expression of ISGs *Cxcl10* and *Gbp2*, as well as IFN-I transcripts (*Ifnb1*), were significantly reduced in cGAS$^{-/-}$ macrophages compared to WT after a 6 hour incubation with B31-A3 (Fig. 2A). In contrast, the levels of *Il-6* and *Tnfa* transcripts were similar in both WT and cGAS$^{-/-}$ BMDMs (Fig. 2B). These results indicate that the cGAS pathway is not a robust trigger for pro-inflammatory cytokines in BMDMs exposed to *B. burgdorferi* and are consistent with the notion that TLR2 or other TLRs sense *B. burgdorferi* ligands to engage NF-κB. Similar results were obtained from protein analysis of cGAS and STING deficient macrophages 9 hours after incubation with B31-A3, with notable reductions in ISGs IFIT1 and ZBP1 in both cGAS$^{-/-}$ and STING$^{gt/gt}$ BMDMs (Fig. 2C). Finally, confocal imaging revealed that *B. burgdorferi* was taken up by BMDMs after a 3 hour incubation (Fig. 2D). Antibody staining against the Outer Surface Protein A (OspA) of *B. burgdorferi* showed coiled, DAPI positive spirochetes in the macrophage cytoplasm, as well as a punctate, DAPI negative OspA staining indicative of bacterial destruction. *B. burgdorferi* OspA also colocalized with the autophagy marker p62/Sequestosome-1 (SQSTM1), suggesting spirochete degradation via macrophage autophagy and/or LC3-associated phagocytosis pathways (74–76). Collectively,

these data indicate that *B. burgdorferi* are taken up by murine macrophages and sensed by the cGAS-STING pathway for engagement of IFN-I responses.

To broaden our findings beyond murine phagocytic cells, we next exposed telomerase immortalized human foreskin fibroblasts (HFF) to *B. burgdorferi* B31-A3. Confocal immunofluorescent imaging with Z-stack reconstitution revealed cell-associated *B. burgdorferi* in the same focal plane with mitochondria (Fig. 3A), suggestive of spirochete internalization. Similar to our results in MEFs, exposure of HFFs to live *B. burgdorferi* increased expression levels of ISGs (*IFI44L*, *IFNB1*) and the pro-inflammatory cytokine gene *TNFA* (Fig. 3B). Although the synthetic TLR2 ligand PAM3CSK4 (Pam3) induced *TNFA* levels comparable to live B31-A3, we did not observe ISG induction, suggesting that *B. burgdorferi* lipoprotein engagement of TLR2 is not responsible for IFN-I responses in HFFs. To examine whether cGAS contributes to IFN-I responses in fibroblasts exposed to *B. burgdorferi*, primary WT and cGAS$^{-/-}$ MEFs were co-cultured with B31-A3 and subjected to qRT-PCR analysis for ISGs and pro-inflammatory transcripts. Consistent with our earlier findings, *B. burgdorferi* induced both ISG and cytokine transcripts in WT MEFs (Fig. 3C). However, the expression of ISGs *Cxcl10* and *Gbp2*, as well as *Ifnb1*, were reduced significantly reduced or entirely abrogated in cGAS$^{-/-}$ MEFs. Although *Il6* transcripts were similar between *B. burgdorferi* exposed WT and cGAS$^{-/-}$ MEFs, *Tnfα* expression was significantly lowered in the absence of cGAS (Fig. 3D). Similar to BMDMs and HFFs, confocal imaging revealed that *B. burgdorferi* was taken up by MEFs after a 6 hour incubation (Fig. 3E). Antibody staining against the OspA lipoprotein of *B. burgdorferi* revealed DAPI positive spirochetes in the MEF cytoplasm, as well as a punctate, DAPI negative OspA staining that colocalized with the autophagy marker p62. Taken together, these data indicate that *B. burgdorferi* can be taken up by fibroblasts where it engages the DNA sensor cGAS.

Additional experiments in STING-deficient MEFs (STING$^{gt/gt}$) revealed markedly reduced *Gbp2* and *Ifnb1* expression, but little change in pro-inflammatory cytokine transcripts, after challenge with *B. burgdorferi* (Fig. S1A-B). Deficiency of the type I interferon receptor (IFNAR) also impaired expression of the ISG *Gbp2*, but did not alter cytokine transcripts, suggesting that ISG induction in MEFs is dependent on autocrine and/or paracrine signaling via IFNAR. In contrast, *B. burgdorferi* infection of Mitochondrial Antiviral Signaling protein null MEFs (MAVS$^{-/-}$), which cannot signal in response to intracellular dsRNA, triggered levels of *Gbp2* and *Ifnb1* mirroring WT cells. This indicates that *B. burgdorferi* co-cultured fibroblasts respond to DNA, not RNA, ligands to induce IFN-I (Fig. S1A). Expression of pro-inflammatory cytokine transcripts *Il6* and *Tnfα* were unchanged or modestly altered in STING$^{gt/gt}$, MAVS$^{-/-}$, and IFNAR$^{-/-}$ MEFs, demonstrating all MEF lines remained responsive to *B. burgdorferi* lipoprotein engagement of TLR2 during co-incubation (Fig. S1B). Moreover, qRT-PCR to detect internal levels of borrelial flagellar gene, *flab*, within host cells revealed roughly equivalent levels of *flaB* among WT and mutant MEF lines (Fig. S1C). This indicates that altered ISG expression in cGAS, STING, and IFNAR deficient cells is not due to changes in the ability of viable *B. burgdorferi* to associate with these MEFs.

cGAS-STING modulates inflammation during *B. burgdorferi* infection in vivo.

To determine roles for the cGAS-STING pathway in borrelial dissemination, tissue colonization, and inflammation during mammalian infection, bioluminescent *B. burgdorferi*, ML23 pBBE22*luc*, was monitored in real time by in vivo imaging in C57BL/6 WT, cGAS$^{-/-}$, and STING$^{gt/gt}$ mice (Fig. 4). Mice were injected with D-luciferin prior to imaging and one mouse in each group was not injected to serve as a bioluminescence background control (Fig. 4A). The

absence of cGAS or STING did not alter the kinetic dissemination of *B. burgdorferi* or the borrelial load as observed in the images and by quantitative analysis of bioluminescence emission (Fig. 4A-B). Outgrowth from infected tissues confirmed the mouse genotypes were equivalently infected with *B. burgdorferi* after 28 days post infection (dpi) (Fig. 4C). To investigate whether the cGAS-STING pathway impacts the development of arthritic phenotypes, tibotarsal joints from WT and cGAS$^{-/-}$ were collected for histopathology (Fig. S2). Consistent with prior reports (77), *B. burgdorferi* induced mild arthritis in WT C57BL/6J mice at 28 days post infection (Fig. S2A). Interestingly, H&E staining revealed that the joints of cGAS$^{-/-}$ mice exhibited reduced synovial papillary hyperplasia and lower joint pathology scores. These results indicate that the cGAS-STING pathway contributes to the development of inflammation during mammalian infection but does not impact the ability of *B. burgdorferi* to readily disseminate and colonize secondary tissues.

DISCUSSION

B. burgdorferi elicits robust innate and adaptive immune responses that involve induction of both IFN-I (IFN-α and β) and IFN-II (IFN-γ) cytokines that drive expression of an overlapping family of interferon-stimulated genes (ISGs) (12, 31, 35, 78, 79). Synovial tissue from patients with post-infection Lyme arthritis expressed ISGs that are associated with both type I and type II interferons (25, 35, 35, 80). Antibody-mediated IFNAR blockade results in a significant reduction in joint inflammation in mice (12), and the inhibition of IFN-γ delays sustained ISG expression and inflammation during *B. burgdorferi* infection (12, 81). A number of prior studies have focused identifying the signaling mechanisms responsible for IFN-I and ISGs elicited by *B. burgdorferi*. Both in vitro and in vivo studies have demonstrated that TLR adaptors MyD88 and TRIF are not the primary contributors to IFN-I induction (12, 13, 22, 82–85). Specifically, in the absence of

TLR2 or TLR5, innate immune receptors that sense lipoproteins or flagella of degraded *B. burgdorferi*, respectively, the induction of ISGs and joint swelling is similar to WT mice (12, 82–84). Studies using human cells have implicated nucleic acid sensing, endosomal localized TLRs (TLR 7, 8, and 9) as regulators of IFN-I induction in human peripheral blood mononuclear cells (PBMCs) challenged with *B. burgdorferi* ex vivo (13, 18, 19, 85). However, TLR9 inhibition does not impair ISG induction in BMDMs exposed to *B. burgdorferi*, in contrast to PBMCs (19, 22, 85). Thus, it is likely that multiple innate immune pathways are responsible for IFN-I induction during *B. burgdorferi* infection. Differences in IFN-I and inflammatory responses across independent studies might also be explained by the use of distinct borrelial strains that vary in invasion and inflammation (11, 86, 87).

Fibroblast and endothelial cells, which do not express a full complement of TLRs, are necessary for *B. burgdorferi* induced IFN-I responses in joints (25, 41). Thus, TLR detection of *B. burgdorferi* nucleic acids is likely not the predominant pathway governing IFN-I responses during *B. burgdorferi* infection in the mammalian host. Therefore, we hypothesized that *B. burgdorferi* might engage an intracellular innate immune pathway leading to IFN-I. Using primary fibroblasts and macrophages from a panel of C57BL/6 mice lacking intracellular nucleic acid sensors or downstream adaptors, we find that the DNA sensing, cGAS-STING pathway is critically required for robust induction of ISGs after exposure to live *B. burgdorferi*. In contrast, we show that deficiency of the main RIG-I-like receptor adaptor MAVS does not impact expression of interferon-stimulated genes or pro-inflammatory transcripts in fibroblasts, indicating that intracellular sensing of *B. burgdorferi* RNA is not a major contributor to IFN-I responses in vitro.

Prior studies have demonstrated the ability of *B. burgdorferi* to become internalized in a variety of phagocytic (macrophages, monocytes, and dendritic cells) and non-phagocytic

(endothelial, fibroblast, and neuroglial cells) cell types during in vitro cultivation (54, 57–62, 88–90). Our immunofluorescent microscopic analyses revealed significant intracellular borrelial OspA staining in BMDMs and mouse and human fibroblasts after short incubations with *B. burgdorferi* B31-A3. In both macrophages and fibroblasts, we observed OspA colocalization with the autophagy marker p62. This substantiates the idea that some spirochetes are taken up into mammalian cells, but also supports the involvement of the cGAS and STING as recent work has revealed that the autophagy machinery is an important regulator of this DNA sensing pathway (91). Moreover, p62 is found in close proximity to TBK1, the kinase necessary for IFN-I induction by STING, and phosphorylation of p62 by TBK1 is important for the negative regulation and turnover of STING (92). We observed coiled and degraded *B. burgdorferi* in BMDMs while intact and degraded spirochetes were observed internalized in mouse and human fibroblasts. However, the phenomenon of host cell internalization by *B. burgdorferi* has not been observed during experimental infection in vivo. Autophagy is linked to the magnitude of host inflammatory responses during *B. burgdorferi* infection (74), and therefore one speculation is the internalization of *B. burgdorferi* during mammalian infection may serve to engage intracellular signaling and perhaps IFN-I or other inflammatory responses, independent of spirochete survival.

The cGAS-STING pathway is a major inducer of IFN-I in response to both exogenous, pathogen-derived DNA, as well as host mitochondrial and nuclear DNA(45, 51, 52, 93–96). cGAS non-discriminately binds double stranded DNA and produces cGAMP that binds and activates STING on the ER. This leads to recruitment and phosphorylation of the kinase TBK1, which phosphorylates and induces nuclear translocation of transcription factors IRF3 or 7 (97). Miller et al demonstrated that *B. burgdorferi* engages IFN-I response genes in an IRF3-dependent manner, further supporting that the signaling machinery downstream of cGAS-STING and other

intracellular nucleic acid sensors is required for ISG induction (12). Numerous intracellular bacterial pathogens, including *Mycobacterium tuberculosis, Listeria monocytogenes,* and *Chlamydia trachomatis*, engage the cGAS-STING axis to induce IFN-I and promote pathogenesis (45, 50, 98–101). More recently, *Pseudomonas aeruginosa* and Group B *Streptococcus* (GBS), extracellular bacterial pathogens, have been shown to trigger IFN-I responses through cGAS-STING in macrophages and dendritic cells(52, 102). Exactly how *B. burgdorferi* and other extracellular bacteria engage cGAS in the cytosol is not entirely clear; however, extracellular bacteria may shed DNA or undergo host-induced membrane damage that liberates bacterial genomic material for uptake and detection. Alternatively, bacterial pathogens can also cause host cell stress, resulting in the release and or accumulation of nuclear or mitochondrial DNA (mtDNA) (103, 104). Mitochondrial stress and mtDNA release, in particular, is linked to innate immune responses through the cGAS-STING axis and is associated with autoimmune disorders (i.e. Lupus and rheumatoid arthritis) and other conditions characterized by elevated IFN-I (94). Thus, it is possible that the IFN-I response induced by *B. burgdorferi* is at least partially dependent on host mtDNA or nuclear DNA sensing. Moreover, it is likely that extracellular *B. burgdorferi* uses distinct mechanisms in phagocytic and non-phagocytic cells to elicit IFN-I responses via the cGAS-STING pathway, and future work is required to reveal the molecular mechanisms at play.

An IFN-I response occurs early in mammalian infection resulting in the development of inflammation and arthritis that persist in part due to IFN-γ during later stages of disease (32, 35, 78, 79). We therefore investigated how absence of cGAS and STING impacted the kinetics of borrelial infection in mice using in vivo imaging to track bioluminescent *B. burgdorferi* in real time through the progression of disease (70, 105). Bioluminescent *B. burgdorferi* was able to successfully disseminate and colonize secondary tissues independently of cGAS or STING.

Inflammation assessed in joints showed a moderate, but significant reduction at 28 dpi in cGAS$^{-/-}$ mice, suggesting that cGAS-STING signaling to IFN-I or other inflammatory response pathways contribute to arthritic phenotypes during *B. burgdorferi* infection. The moderate phenotype observed in cGAS$^{-/-}$ joints is likely attributed to the C57BL/6 inbred background. However, these experiments are the first to explore roles for the cGAS STING pathway in mammalian infection. It is important to note that the absence of cGAS did not eliminate inflammation entirely, indicating that *B. burgdorferi* associated arthritis is multifactorial and involves additional innate and adaptive immune pathways as have been reported by others (13, 17, 19, 20, 85).

While this study is impactful in that it is the first to link the cGAS-STING pathway to *B. burgdorferi* induced IFN-I responses, it is not without limitations. C3H is the preferred model for borrelial infection because this background develops inflammation and pathologic disease at a significantly higher level than C57BL/6 or Balb/c mice (34, 77). An elegant study identified the *Bbaa1* locus in C3H mice responsible for IFN-I responses observed during borrelial infection and showed that introduction of this locus into C57BL/6 mice yielded similar inflammatory responses to C3H (29). Our study employed WT, cGAS, and STING knockout strains on a pure C57BL/6 background as they are commercially available and well-characterized. We employed highly invasive and inflammatory RST1 *B. burgdorferi* B31-A3 for our studies and were able to observe IFN-I induction even in cells from the C57BL/6 background. These responses were markedly attenuated or lost when using sonicated *B. burgdorferi* B31-A3. Other studies have revealed weak or absent ISG expression during in vitro challenge with *B. burgdorferi*, although most utilized sonicated bacteria or less inflammatory RST3 strains (12, 22, 77, 82). This indicates that the C57BL/6 background is not devoid of IFN-I responsiveness to borrelial infection. Our work and previous studies show C57BL/6 mice and cell lines do produce measurable IFN-I and

inflammatory responses to borrelial infection, and therefore we propose it is an appropriate model for this initial characterization of cGAS-STING in the innate immune response to *B. burgdorferi* (12). However, the development of cGAS or STING knockout lines on the C3H background will be necessary to fully characterize the role of this innate immune pathway in *B. burgdorferi* infection dynamics, tissue-specific inflammation, and arthritic phenotypes in vivo.

In conclusion, our study is the first to show that *B. burgdorferi* triggers the intracellular cGAS-STING DNA sensing pathway that governs IFN-I responses. Future studies are needed to investigate the how borrelial cells initiate IFN-I responses through this pathway by characterizing the source of DNA that binds to cGAS (i.e. bacterial or host) and determining whether borrelial internalization is required. The absence of cGAS or STING does not appear to alter *B. burgdorferi* dissemination or its ability to colonize secondary tissues, but studies in C3H mice lacking this innate immune pathway may reveal differential bacterial kinetics and/or inflammatory responses that do impact the course of infection. Additional work to clarify these open questions may support the development cGAS- and/or STING-based immunotherapeutics that may be effective against active infection or persistent symptoms of *B. burgdorferi*, such as Lyme arthritis.

ACKNOWLEDGEMENTS

We thank members of the Hyde and West labs for helpful discussions. We thank Dr. Jon Skare for providing the OspA antibody.

DISCLOSURES

The authors have no financial conflicts of interest.

REFERENCES

1. Steere, A. C., F. Strle, G. P. Wormser, L. T. Hu, J. A. Branda, J. W. R. Hovius, X. Li, and P. S. Mead. 2016. Lyme borreliosis. *Nat. Rev. Dis. Primer* 2: 16090.

2. Stanek, G., and F. Strle. 2018. Lyme borreliosis–from tick bite to diagnosis and treatment. *FEMS Microbiol. Rev.* 42: 233–258.

3. Radolf, J. D., M. J. Caimano, B. Stevenson, and L. T. Hu. 2012. Of ticks, mice and men: understanding the dual-host lifestyle of Lyme disease spirochaetes. *Nat. Rev. Microbiol.* 10: 87–99.

4. Shapiro, E. D. 2014. Lyme disease. *N. Engl. J. Med.* 371: 684.

5. Kugeler, K. J., A. M. Schwartz, M. J. Delorey, P. S. Mead, and A. F. Hinckley. Estimating the Frequency of Lyme Disease Diagnoses, United States, 2010–2018 - Volume 27, Number 2—February 2021 - Emerging Infectious Diseases journal - CDC. .

6. Mead, P. S. 2015. Epidemiology of Lyme disease. *Infect. Dis. Clin. North Am.* 29: 187–210.

7. Schwartz, A. M. 2017. Surveillance for Lyme Disease — United States, 2008–2015. *MMWR Surveill. Summ.* 66.

8. Radolf, J. D., K. Strle, J. E. Lemieux, and F. Strle. 2021. Lyme Disease in Humans. *Curr. Issues Mol. Biol.* 42: 333–384.

9. Bamm, V. V., J. T. Ko, I. L. Mainprize, V. P. Sanderson, and M. K. B. Wills. 2019. Lyme Disease Frontiers: Reconciling Borrelia Biology and Clinical Conundrums. *Pathog. Basel Switz.* 8: E299.

10. Khatchikian, C. E., R. B. Nadelman, J. Nowakowski, I. Schwartz, M. Z. Levy, D. Brisson, and G. P. Wormser. 2015. Public health impact of strain specific immunity to Borrelia burgdorferi. *BMC Infect. Dis.* 15: 472.

11. Strle, K., K. L. Jones, E. E. Drouin, X. Li, and A. C. Steere. 2011. Borrelia burgdorferi RST1 (OspC type A) genotype is associated with greater inflammation and more severe Lyme disease. *Am. J. Pathol.* 178: 2726–2739.

12. Miller, J. C., Y. Ma, J. Bian, K. C. F. Sheehan, J. F. Zachary, J. H. Weis, R. D. Schreiber, and J. J. Weis. 2008. A critical role for type I IFN in arthritis development following Borrelia burgdorferi infection of mice. *J. Immunol. Baltim. Md 1950* 181: 8492–8503.

13. Cervantes, J. L., S. M. Dunham-Ems, C. J. La Vake, M. M. Petzke, B. Sahay, T. J. Sellati, J. D. Radolf, and J. C. Salazar. 2011. Phagosomal signaling by Borrelia burgdorferi in human monocytes involves Toll-like receptor (TLR) 2 and TLR8 cooperativity and TLR8-mediated induction of IFN-beta. *Proc. Natl. Acad. Sci. U. S. A.* 108: 3683–3688.

14. Wooten, R. M., M. A. Ying, R. A. Yoder, J. P. Brown, J. H. Weis, J. F. Zachary, C. J. Kirschning, and J. J. Weis. 2002. Toll-like receptor 2 plays a pivotal role in host defense and inflammatory response to Borrelia burgdorferi. *Vector Borne Zoonotic Dis* 2: 275–8.

15. Marre, M. L., T. Petnicki-Ocwieja, A. S. DeFrancesco, C. T. Darcy, and L. T. Hu. 2010. Human integrin α(3)β(1) regulates TLR2 recognition of lipopeptides from endosomal compartments. *PloS One* 5: e12871.

16. Dennis, V. A., S. Dixit, S. M. O'Brien, X. Alvarez, B. Pahar, and M. T. Philipp. 2009. Live Borrelia burgdorferi spirochetes elicit inflammatory mediators from human monocytes via the Toll-like receptor signaling pathway. *Infect. Immun.* 77: 1238–1245.

17. Shin, O. S., R. R. Isberg, S. Akira, S. Uematsu, A. K. Behera, and L. T. Hu. 2008. Distinct roles for MyD88 and Toll-like receptors 2, 5, and 9 in phagocytosis of Borrelia burgdorferi and cytokine induction. *Infect. Immun.* 76: 2341–2351.

18. Cervantes, J. L., C. J. La Vake, B. Weinerman, S. Luu, C. O'Connell, P. H. Verardi, and J. C. Salazar. 2013. Human TLR8 is activated upon recognition of Borrelia burgdorferi RNA in the phagosome of human monocytes. *J. Leukoc. Biol.* 94: 1231–1241.

19. Petzke, M. M., A. Brooks, M. A. Krupna, D. Mordue, and I. Schwartz. 2009. Recognition of Borrelia burgdorferi, the Lyme disease spirochete, by TLR7 and TLR9 induces a type I IFN response by human immune cells. *J. Immunol. Baltim. Md 1950* 183: 5279–5292.

20. Parthasarathy, G., and M. T. Philipp. 2018. Intracellular TLR7 is activated in human oligodendrocytes in response to Borrelia burgdorferi exposure. *Neurosci. Lett.* 671: 38–42.

21. Krupna-Gaylord, M. A., D. Liveris, A. C. Love, G. P. Wormser, I. Schwartz, and M. M. Petzke. 2014. Induction of type I and type III interferons by Borrelia burgdorferi correlates with pathogenesis and requires linear plasmid 36. *PloS One* 9: e100174.

22. Miller, J. C., H. Maylor-Hagen, Y. Ma, J. H. Weis, and J. J. Weis. 2010. The Lyme disease spirochete Borrelia burgdorferi utilizes multiple ligands, including RNA, for interferon regulatory factor 3-dependent induction of type I interferon-responsive genes. *Infect. Immun.* 78: 3144–3153.

23. Hastey, C. J., J. Ochoa, K. J. Olsen, S. W. Barthold, and N. Baumgarth. 2014. MyD88- and TRIF-independent induction of type I interferon drives naive B cell accumulation but not loss of lymph node architecture in Lyme disease. *Infect. Immun.* 82: 1548–1558.

24. Salazar, J. C., S. Duhnam-Ems, C. La Vake, A. R. Cruz, M. W. Moore, M. J. Caimano, L. Velez-Climent, J. Shupe, W. Krueger, and J. D. Radolf. 2009. Activation of human monocytes by live Borrelia burgdorferi generates TLR2-dependent and -independent responses which include induction of IFN-beta. *PLoS Pathog.* 5: e1000444.

25. Lochhead, R. B., F. L. Sonderegger, Y. Ma, J. E. Brewster, D. Cornwall, H. Maylor-Hagen, J. C. Miller, J. F. Zachary, J. H. Weis, and J. J. Weis. 2012. Endothelial cells and fibroblasts amplify

the arthritogenic type I IFN response in murine Lyme disease and are major sources of chemokines in Borrelia burgdorferi-infected joint tissue. *J. Immunol. Baltim. Md 1950* 189: 2488–2501.

26. Bernard, Q., M. Thakur, A. A. Smith, C. Kitsou, X. Yang, and U. Pal. 2019. Borrelia burgdorferi protein interactions critical for microbial persistence in mammals. *Cell. Microbiol.* 21: e12885.

27. Meddeb, M., W. Carpentier, N. Cagnard, S. Nadaud, A. Grillon, C. Barthel, S. J. De Martino, B. Jaulhac, N. Boulanger, and F. Schramm. 2016. Homogeneous Inflammatory Gene Profiles Induced in Human Dermal Fibroblasts in Response to the Three Main Species of Borrelia burgdorferi sensu lato. *PloS One* 11: e0164117.

28. Berner, A., M. Bachmann, J. Pfeilschifter, P. Kraiczy, and H. Mühl. 2015. Interferon-α curbs production of interleukin-22 by human peripheral blood mononuclear cells exposed to live Borrelia burgdorferi. *J. Cell. Mol. Med.* 19: 2507–2511.

29. Ma, Y., K. K. C. Bramwell, R. B. Lochhead, J. K. Paquette, J. F. Zachary, J. H. Weis, C. Teuscher, and J. J. Weis. 2014. *Borrelia burgdorferi* Arthritis–Associated Locus *Bbaa1* Regulates Lyme Arthritis and K/B×N Serum Transfer Arthritis through Intrinsic Control of Type I IFN Production. *J. Immunol.* 193: 6050–6060.

30. Jacek, E., B. A. Fallon, A. Chandra, M. K. Crow, G. P. Wormser, and A. Alaedini. 2013. Increased IFNα activity and differential antibody response in patients with a history of Lyme disease and persistent cognitive deficits. *J. Neuroimmunol.* 255: 85–91.

31. Marques, A., I. Schwartz, G. P. Wormser, Y. Wang, R. L. Hornung, C. Y. Demirkale, P. J. Munson, S.-P. Turk, C. Williams, C.-C. R. Lee, J. Yang, and M. M. Petzke. 2017. Transcriptome Assessment of Erythema Migrans Skin Lesions in Patients With Early Lyme Disease Reveals Predominant Interferon Signaling. *J. Infect. Dis.* 217: 158–167.

32. Petzke, M., and I. Schwartz. 2015. Borrelia burgdorferi Pathogenesis and the Immune Response. *Clin. Lab. Med.* 35: 745–764.

33. Paquette, J. K., Y. Ma, C. Fisher, J. Li, S. B. Lee, J. F. Zachary, Y. S. Kim, C. Teuscher, and J. J. Weis. 2017. Genetic Control of Lyme Arthritis by Borrelia burgdorferi Arthritis-Associated Locus 1 Is Dependent on Localized Differential Production of IFN-β and Requires Upregulation of Myostatin. *J. Immunol. Baltim. Md 1950* 199: 3525–3534.

34. Barthold, S. W., D. S. Beck, G. M. Hansen, G. A. Terwilliger, and K. D. Moody. 1990. Lyme borreliosis in selected strains and ages of laboratory mice. *J Infect Dis* 162: 133–8.

35. Lochhead, R. B., S. L. Arvikar, J. M. Aversa, R. I. Sadreyev, K. Strle, and A. C. Steere. 2019. Robust interferon signature and suppressed tissue repair gene expression in synovial tissue from patients with postinfectious, Borrelia burgdorferi-induced Lyme arthritis. *Cell. Microbiol.* 21: e12954.

36. Mason, L. M. K., A. Wagemakers, C. van ’t Veer, A. Oei, W. J. van der Pot, K. Ahmed, T. van der Poll, T. B. H. Geijtenbeek, and J. W. R. Hovius. 2016. Borrelia burgdorferi Induces TLR2-Mediated Migration of Activated Dendritic Cells in an Ex Vivo Human Skin Model. *PloS One* 11: e0164040.

37. Oosting, M., H. Ter Hofstede, P. Sturm, G. J. Adema, B.-J. Kullberg, J. W. M. van der Meer, M. G. Netea, and L. A. B. Joosten. 2011. TLR1/TLR2 heterodimers play an important role in the recognition of Borrelia spirochetes. *PloS One* 6: e25998.

38. Salazar, J. C., C. D. Pope, M. W. Moore, J. Pope, T. G. Kiely, and J. D. Radolf. 2005. Lipoprotein-dependent and -independent immune responses to spirochetal infection. *Clin. Diagn. Lab. Immunol.* 12: 949–958.

39. Barbalat, R., L. Lau, R. M. Locksley, and G. M. Barton. 2009. Toll-like receptor 2 on inflammatory monocytes induces type I interferon in response to viral but not bacterial ligands. *Nat. Immunol.* 10: 1200–1207.

40. Oosenbrug, T., M. J. van de Graaff, M. C. Haks, S. van Kasteren, and M. E. Ressing. 2020. An alternative model for type I interferon induction downstream of human TLR2. *J. Biol. Chem.* 295: 14325–14342.

41. Kawasaki, T., and T. Kawai. 2014. Toll-like receptor signaling pathways. *Front. Immunol.* 5: 461.

42. Cai, X., Y.-H. Chiu, and Z. J. Chen. 2014. The cGAS-cGAMP-STING pathway of cytosolic DNA sensing and signaling. *Mol. Cell* 54: 289–296.

43. Liu, S., X. Cai, J. Wu, Q. Cong, X. Chen, T. Li, F. Du, J. Ren, Y.-T. Wu, N. V. Grishin, and Z. J. Chen. 2015. Phosphorylation of innate immune adaptor proteins MAVS, STING, and TRIF induces IRF3 activation. *Science* 347: aaa2630.

44. Patrick, K. L., S. L. Bell, and R. O. Watson. 2016. For Better or Worse: Cytosolic DNA Sensing during Intracellular Bacterial Infection Induces Potent Innate Immune Responses. *J. Mol. Biol.* 428: 3372–3386.

45. Watson, R. O., S. L. Bell, D. A. MacDuff, J. M. Kimmey, E. J. Diner, J. Olivas, R. E. Vance, C. L. Stallings, H. W. Virgin, and J. S. Cox. 2015. The cytosolic sensor cGAS detects Mycobacterium tuberculosis DNA to induce type I interferons and activate autophagy. *Cell Host Microbe* 17: 811–819.

46. Gao, D., J. Wu, Y.-T. Wu, F. Du, C. Aroh, N. Yan, L. Sun, and Z. J. Chen. 2013. Cyclic GMP-AMP synthase is an innate immune sensor of HIV and other retroviruses. *Science* 341: 903–906.

47. Castanier, C., N. Zemirli, A. Portier, D. Garcin, N. Bidère, A. Vazquez, and D. Arnoult. 2012. MAVS ubiquitination by the E3 ligase TRIM25 and degradation by the proteasome is involved in type I interferon production after activation of the antiviral RIG-I-like receptors. *BMC Biol.* 10: 44.

48. Seth, R. B., L. Sun, C.-K. Ea, and Z. J. Chen. 2005. Identification and Characterization of MAVS, a Mitochondrial Antiviral Signaling Protein that Activates NF-κB and IRF3. *Cell* 122: 669–682.

49. Kawai, T., K. Takahashi, S. Sato, C. Coban, H. Kumar, H. Kato, K. J. Ishii, O. Takeuchi, and S. Akira. 2005. IPS-1, an adaptor triggering RIG-I- and Mda5-mediated type I interferon induction. *Nat. Immunol.* 6: 981–988.

50. Hansen, K., T. Prabakaran, A. Laustsen, S. E. Jørgensen, S. H. Rahbæk, S. B. Jensen, R. Nielsen, J. H. Leber, T. Decker, K. A. Horan, M. R. Jakobsen, and S. R. Paludan. 2014. Listeria monocytogenes induces IFNβ expression through an IFI16-, cGAS- and STING-dependent pathway. *EMBO J.* 33: 1654–1666.

51. Liu, N., X. Pang, H. Zhang, and P. Ji. 2022. The cGAS-STING Pathway in Bacterial Infection and Bacterial Immunity. *Front. Immunol.* 12.

52. Zhou, C., B. Wang, Q. Wu, P. Lin, S. Qin, Q. Pu, X. Yu, and M. Wu. 2021. Identification of cGAS as an innate immune sensor of extracellular bacterium Pseudomonas aeruginosa. *iScience* 24: 101928.

53. Liu, H., P. Moura-Alves, G. Pei, H.-J. Mollenkopf, R. Hurwitz, X. Wu, F. Wang, S. Liu, M. Ma, Y. Fei, C. Zhu, A.-B. Koehler, D. Oberbeck-Mueller, K. Hahnke, M. Klemm, U. Guhlich-Bornhof, B. Ge, A. Tuukkanen, M. Kolbe, A. Dorhoi, and S. H. Kaufmann. 2019. cGAS facilitates sensing of extracellular cyclic dinucleotides to activate innate immunity. *EMBO Rep.* 20: e46293.

54. Wu, J., E. H. Weening, J. B. Faske, M. Höök, and J. T. Skare. 2011. Invasion of Eukaryotic Cells by Borrelia burgdorferi Requires β1 Integrins and Src Kinase Activity. *Infect. Immun.* 79: 1338–1348.

55. Woitzik, P., and S. Linder. 2021. Molecular Mechanisms of Borrelia burgdorferi Phagocytosis and Intracellular Processing by Human Macrophages. *Biology* 10: 567.

56. Carreras-González, A., D. Barriales, A. Palacios, M. Montesinos-Robledo, N. Navasa, M. Azkargorta, A. Peña-Cearra, J. Tomás-Cortázar, I. Escobes, M. A. Pascual-Itoiz, J. Hradiská, J. Kopecký, D. Gil-Carton, R. Prados-Rosales, L. Abecia, E. Atondo, I. Martín, A. Pellón, F. Elortza, H. Rodríguez, and J. Anguita. 2019. Regulation of macrophage activity by surface receptors contained within Borrelia burgdorferi-enriched phagosomal fractions. *PLoS Pathog.* 15: e1008163.

57. Williams, S. K., Z. P. Weiner, and R. D. Gilmore. 2018. Human neuroglial cells internalize Borrelia burgdorferi by coiling phagocytosis mediated by Daam1. *PloS One* 13: e0197413.

58. Killpack, T. L., M. Ballesteros, S. C. Bunnell, A. Bedugnis, L. Kobzik, L. T. Hu, and T. Petnicki-Ocwieja. 2017. Phagocytic Receptors Activate Syk and Src Signaling during Borrelia burgdorferi Phagocytosis. *Infect. Immun.* 85: e00004-17.

59. Petnicki-Ocwieja, T., and A. Kern. 2014. Mechanisms of Borrelia burgdorferi internalization and intracellular innate immune signaling. *Front. Cell. Infect. Microbiol.* 4: 175.

60. Cruz, A. R., M. W. Moore, C. J. L. Vake, C. H. Eggers, J. C. Salazar, and J. D. Radolf. 2008. Phagocytosis of Borrelia burgdorferi, the Lyme Disease Spirochete, Potentiates Innate Immune Activation and Induces Apoptosis in Human Monocytes. *Infect. Immun.* 76: 56–70.

61. Livengood, J. A., and Jr. Gilmore. November. Invasion of human neuronal and glial cells by an infectious strain of Borrelia burgdorferi. *Microbes Infect.* 8: 2832–2840.

62. Ma, Y., A. Sturrock, and J. J. Weis. 1991. Intracellular localization of Borrelia burgdorferi within human endothelial cells. *Infect Immun* 59: 671–8.

63. Burdette, D. L., K. M. Monroe, K. Sotelo-Troha, J. S. Iwig, B. Eckert, M. Hyodo, Y. Hayakawa, and R. E. Vance. 2011. STING is a direct innate immune sensor of cyclic di-GMP. *Nature* 478: 515–518.

64. Rogers, E. A., D. Terekhova, H.-M. Zhang, K. M. Hovis, I. Schwartz, and R. T. Marconi. 2009. Rrp1, a cyclic-di-GMP-producing response regulator, is an important regulator of Borrelia burgdorferi core cellular functions. *Mol. Microbiol.* 71: 1551–1573.

65. Caimano, M. J., S. Dunham-Ems, A. M. Allard, M. B. Cassera, M. Kenedy, and J. D. Radolf. 2015. c-di-GMP modulates gene expression in Lyme disease spirochetes at the tick-mammal interface to promote spirochete survival during the blood meal and tick-to-mammal transmission. *Infect. Immun.* .

66. Savage, C. R., W. K. Arnold, A. Gjevre-Nail, B. J. Koestler, E. L. Bruger, J. R. Barker, C. M. Waters, and B. Stevenson. 2015. Intracellular Concentrations of Borrelia burgdorferi Cyclic Di-AMP Are Not Changed by Altered Expression of the CdaA Synthase. *PloS One* 10: e0125440.

67. Barbour, A. G. 1984. Isolation and cultivation of Lyme disease spirochetes. *Yale J Biol Med* 57: 521–5.

68. Zückert, W. R. 2007. Laboratory maintenance of Borrelia burgdorferi. *Curr. Protoc. Microbiol.* Chapter 12: Unit 12C.1.

69. Labandeira-Rey, M., and J. T. Skare. 2001. Decreased infectivity in Borrelia burgdorferi strain B31 is associated with loss of linear plasmid 25 or 28-1. *Infect Immun* 69: 446–55.

70. Hyde, J. A., E. H. Weening, M. Chang, J. P. Trzeciakowski, M. Höök, J. D. Cirillo, and J. T. Skare. 2011. Bioluminescent imaging of Borrelia burgdorferi in vivo demonstrates that the

fibronectin-binding protein BBK32 is required for optimal infectivity. *Mol. Microbiol.* 82: 99–113.

71. Elias, A. F., P. E. Stewart, D. Grimm, M. J. Caimano, C. H. Eggers, K. Tilly, J. L. Bono, D. R. Akins, J. D. Radolf, T. G. Schwan, and P. Rosa. 2002. Clonal polymorphism of Borrelia burgdorferi strain B31 MI: implications for mutagenesis in an infectious strain background. *Infect Immun* 70: 2139–50.

72. Torres-Odio, S., Y. Lei, S. Gispert, A. Maletzko, J. Key, S. S. Menissy, I. Wittig, G. Auburger, and A. P. West. 2021. Loss of Mitochondrial Protease CLPP Activates Type I IFN Responses through the Mitochondrial DNA-cGAS-STING Signaling Axis. *J. Immunol. Baltim. Md 1950* 206: 1890–1900.

73. Skare, J. T., D. K. Shaw, J. P. Trzeciakowski, and J. A. Hyde. 2016. In Vivo Imaging Demonstrates That Borrelia burgdorferi ospC Is Uniquely Expressed Temporally and Spatially throughout Experimental Infection. *PloS One* 11: e0162501.

74. Buffen, K., M. Oosting, S. Mennens, P. K. Anand, T. S. Plantinga, P. Sturm, F. L. van de Veerdonk, J. W. M. van der Meer, R. J. Xavier, T.-D. Kanneganti, M. G. Netea, and L. A. B. Joosten. 2013. Autophagy modulates Borrelia burgdorferi-induced production of interleukin-1β (IL-1β). *J. Biol. Chem.* 288: 8658–8666.

75. Buffen, K., M. Oosting, Y. Li, T.-D. Kanneganti, M. G. Netea, and L. A. B. Joosten. 2016. Autophagy suppresses host adaptive immune responses toward Borrelia burgdorferi. *J. Leukoc. Biol.* 100: 589–598.

76. Grijmans, B. J. M., S. B. van der Kooij, M. Varela, and A. H. Meijer. 2022. LAPped in Proof: LC3-Associated Phagocytosis and the Arms Race Against Bacterial Pathogens. *Front. Cell. Infect. Microbiol.* 11.

77. Ma, Y., K. P. Seiler, E. J. Eichwald, J. H. Weis, C. Teuscher, and J. J. Weis. 1998. Distinct characteristics of resistance to Borrelia burgdorferi-induced arthritis in C57BL/6N mice. *Infect. Immun.* 66: 161–168.

78. Lochhead, R. B., D. Ordoñez, S. L. Arvikar, J. M. Aversa, L. S. Oh, B. Heyworth, R. Sadreyev, A. C. Steere, and K. Strle. 2019. Interferon-gamma production in Lyme arthritis synovial tissue promotes differentiation of fibroblast-like synoviocytes into immune effector cells. *Cell. Microbiol.* 21: e12992.

79. Petzke, M. M., R. Iyer, A. C. Love, Z. Spieler, A. Brooks, and I. Schwartz. 2016. Borrelia burgdorferi induces a type I interferon response during early stages of disseminated infection in mice. *BMC Microbiol.* 16: 29.

80. Shin, J. J., L. J. Glickstein, and A. C. Steere. 2007. High levels of inflammatory chemokines and cytokines in joint fluid and synovial tissue throughout the course of antibiotic-refractory lyme arthritis. *Arthritis Rheum.* 56: 1325–1335.

81. Brown, C. R., and S. L. Reiner. 1999. Genetic control of experimental lyme arthritis in the absence of specific immunity. *Infect. Immun.* 67: 1967–1973.

82. Bolz, D. D., R. S. Sundsbak, Y. Ma, S. Akira, C. J. Kirschning, J. F. Zachary, J. H. Weis, and J. J. Weis. 2004. MyD88 plays a unique role in host defense but not arthritis development in Lyme disease. *J. Immunol. Baltim. Md 1950* 173: 2003–2010.

83. Behera, A. K., E. Hildebrand, J. Szafranski, H.-H. Hung, A. J. Grodzinsky, R. Lafyatis, A. E. Koch, R. Kalish, G. Perides, A. C. Steere, and L. T. Hu. 2006. Role of aggrecanase 1 in Lyme arthritis. *Arthritis Rheum.* 54: 3319–3329.

84. Liu, N., R. R. Montgomery, S. W. Barthold, and L. K. Bockenstedt. 2004. Myeloid differentiation antigen 88 deficiency impairs pathogen clearance but does not alter inflammation in Borrelia burgdorferi-infected mice. *Infect Immun* 72: 3195–203.

85. Love, A. C., I. Schwartz, and M. M. Petzke. 2014. Borrelia burgdorferi RNA induces type I and III interferons via Toll-like receptor 7 and contributes to production of NF-κB-dependent cytokines. *Infect. Immun.* 82: 2405–2416.

86. Jones, K. L., G. A. McHugh, L. J. Glickstein, and A. C. Steere. 2009. Analysis of Borrelia burgdorferi genotypes in patients with Lyme arthritis: High frequency of ribosomal RNA intergenic spacer type 1 strains in antibiotic-refractory arthritis. *Arthritis Rheum.* 60: 2174–2182.

87. Mason, L. M. K., E. A. Herkes, M. A. Krupna-Gaylord, A. Oei, T. van der Poll, G. P. Wormser, I. Schwartz, M. M. Petzke, and J. W. R. Hovius. 2015. Borrelia burgdorferi clinical isolates induce human innate immune responses that are not dependent on genotype. *Immunobiology* 220: 1141–1150.

88. Hawley, K., N. Navasa, C. M. Olson, T. C. Bates, R. Garg, M. N. Hedrick, D. Conze, M. Rincón, and J. Anguita. 2012. Macrophage p38 Mitogen-Activated Protein Kinase Activity Regulates Invariant Natural Killer T-Cell Responses During Borrelia burgdorferi Infection. *J. Infect. Dis.* 206: 283–291.

89. Filgueira, L., F. O. Nestle, M. Rittig, H. I. Joller, and P. Groscurth. 1996. Human dendritic cells phagocytose and process Borrelia burgdorferi. *J. Immunol.* 157: 2998–3005.

90. Naj, X., A.-K. Hoffmann, M. Himmel, and S. Linder. 2013. The formins FMNL1 and mDia1 regulate coiling phagocytosis of Borrelia burgdorferi by primary human macrophages. *Infect. Immun.* 81: 1683–1695.

91. Zhang, K., S. Wang, H. Gou, J. Zhang, and C. Li. 2021. Crosstalk Between Autophagy and the cGAS–STING Signaling Pathway in Type I Interferon Production. *Front. Cell Dev. Biol.* 9.

92. Prabakaran, T., C. Bodda, C. Krapp, B.-C. Zhang, M. H. Christensen, C. Sun, L. Reinert, Y. Cai, S. B. Jensen, M. K. Skouboe, J. R. Nyengaard, C. B. Thompson, R. J. Lebbink, G. C. Sen, G. van Loo, R. Nielsen, M. Komatsu, L. N. Nejsum, M. R. Jakobsen, M. Gyrd-Hansen, and S. R. Paludan. 2018. Attenuation of cGAS-STING signaling is mediated by a p62/SQSTM1-dependent autophagy pathway activated by TBK1. *EMBO J.* 37: e97858.

93. West, A. P., W. Khoury-Hanold, M. Staron, M. C. Tal, C. M. Pineda, S. M. Lang, M. Bestwick, B. A. Duguay, N. Raimundo, D. A. MacDuff, S. M. Kaech, J. R. Smiley, R. E. Means, A. Iwasaki, and G. S. Shadel. 2015. Mitochondrial DNA stress primes the antiviral innate immune response. *Nature* 520: 553–557.

94. West, A. P., and G. S. Shadel. 2017. Mitochondrial DNA in innate immune responses and inflammatory pathology. *Nat. Rev. Immunol.* 17: 363–375.

95. Wang, H., C. Zang, M. Ren, M. Shang, Z. Wang, X. Peng, Q. Zhang, X. Wen, Z. Xi, and C. Zhou. 2020. Cellular uptake of extracellular nucleosomes induces innate immune responses by binding and activating cGMP-AMP synthase (cGAS). *Sci. Rep.* 10: 15385.

96. Choudhuri, S., and N. J. Garg. 2020. PARP1-cGAS-NF-κB pathway of proinflammatory macrophage activation by extracellular vesicles released during Trypanosoma cruzi infection and Chagas disease. *PLoS Pathog.* 16: e1008474.

97. Ablasser, A., and Z. J. Chen. 2019. cGAS in action: Expanding roles in immunity and inflammation. *Science* 363: eaat8657.

98. Zhang, Y., L. Yeruva, A. Marinov, D. Prantner, P. B. Wyrick, V. Lupashin, and U. M. Nagarajan. 2014. The DNA sensor, cyclic GMP-AMP synthase, is essential for induction of IFN-β during Chlamydia trachomatis infection. *J. Immunol. Baltim. Md 1950* 193: 2394–2404.

99. Nandakumar, R., R. Tschismarov, F. Meissner, T. Prabakaran, A. Krissanaprasit, E. Farahani, B.-C. Zhang, S. Assil, A. Martin, W. Bertrams, C. K. Holm, A. Ablasser, T. Klause, M. K. Thomsen, B. Schmeck, K. A. Howard, T. Henry, K. V. Gothelf, T. Decker, and S. R. Paludan. 2019. Intracellular bacteria engage a STING-TBK1-MVB12b pathway to enable paracrine cGAS-STING signalling. *Nat. Microbiol.* 4: 701–713.

100. Webster, S. J., S. Brode, L. Ellis, T. J. Fitzmaurice, M. J. Elder, N. O. Gekara, P. Tourlomousis, C. Bryant, S. Clare, R. Chee, H. J. S. Gaston, and J. C. Goodall. 2017. Detection of a microbial metabolite by STING regulates inflammasome activation in response to Chlamydia trachomatis infection. *PLoS Pathog.* 13: e1006383.

101. Su, X., H. Xu, M. French, Y. Zhao, L. Tang, X.-D. Li, J. Chen, and G. Zhong. 2022. Evidence for cGAS-STING Signaling in the Female Genital Tract Resistance to Chlamydia trachomatis Infection. *Infect. Immun.* 90: e0067021.

102. Andrade, W. A., A. Firon, T. Schmidt, V. Hornung, K. A. Fitzgerald, E. A. Kurt-Jones, P. Trieu-Cuot, D. T. Golenbock, and P.-A. Kaminski. 2016. Group B Streptococcus Degrades Cyclic-di-AMP to Modulate STING-Dependent Type I Interferon Production. *Cell Host Microbe* 20: 49–59.

103. Kausar, S., L. Yang, M. N. Abbas, X. Hu, Y. Zhao, Y. Zhu, and H. Cui. 2020. Mitochondrial DNA: A Key Regulator of Anti-Microbial Innate Immunity. *Genes* 11: 86.

104. Gao, Y., W. Xu, X. Dou, H. Wang, X. Zhang, S. Yang, H. Liao, X. Hu, and H. Wang. 2019. Mitochondrial DNA Leakage Caused by Streptococcus pneumoniae Hydrogen Peroxide Promotes Type I IFN Expression in Lung Cells. *Front. Microbiol.* 10.

105. Hyde, J. A., and J. T. Skare. 2018. Detection of Bioluminescent Borrelia burgdorferi from In Vitro Cultivation and During Murine Infection. *Methods Mol. Biol. Clifton NJ* 1690: 241–257.

TABLES

Table I. – Oligonucleotide sequences used in the study.

Gene	Forward Primer Sequence	Reverse Primer Sequence
Mouse		
Bactin	5’-TTCTTTGCAGCTCCTTCGTT-3’	5’-ATGGAGGGGAATACAGCCC-3’
Cxcl10	5’-CCAAGTGCTGCCGTCATTTTC-3’	5’-GGCTCGCAGGGATGATTTCAA-3’
Gbp2	5’-CAGCATAGGAACCATCAACCA-3’	5’-TCTACCCCACTCTGGTCAGG-3’
Ifit3	5’-CAGCATAGGAACCATCAACCA-3’	5’-TCTACCCCACTCTGGTCAGG-3’
Ifnb1	5’-CCCTATGGAGATGACGGAGA-3’	5’-CCCAGTGCTGGAGAAATTGT-3’
Il6	5’-TGATGCACTTGCAGAAAACA-3’	5’-ACCAGAGGAAATTTTCAATAGGC-3’
Tnfa	5’-CCACCACGCTCTTCTGTCTAC-3’	5’-AGGGTCTGGGCCATAGAACT-3’
Human		
GAPDH	5’-AGCCACATCGCTCAGACA-3’	5’-GCCCAATACGACCAAATCC-3’
IFNB1	5’-CTTTCGAAGCCTTTGCTCTG-3’	5’-CAGGAGAGCAATTTGGAGGA-3’
IFI44L	5’-CAATTTAAGCCTGATCTAACCCC-3’	5’-CAGTTGCGCAGATGATTTTC-3’
TNFA	5’-CTGCTGCACTTTGGAGTGAT-3'	5’-AGATGATCTGACTGCCTGGG-3'
B. burgdorferi		
flaB	5’-CAGCTAATGTTGCAAATCTTTTCTCT-3’	5’-TTCCTGTTGAACACCCTCTTGA-3’

Table II – Antibodies used in the study.

Antibody	**Source**	**Catalogue number**	**Dilution**
αTubulin	DSHB	12G10	1:5,000
cGAS	Cell Signaling	31659	1:1,000
Ifit1	gift from G.Sen at Cleveland Clinic		1:1,000
Zbp1	Adipogen	AG-20B-0010	1:1,000
Sting	Proteintech	19851-1-AP	1:1,000
OspA	Capicorn	BOR-018-48310	1:1,000,000
p62	Proteintech	18420-1-AP	1:500
Hsp60	Santa Cruz	sc-1052	1:5,000

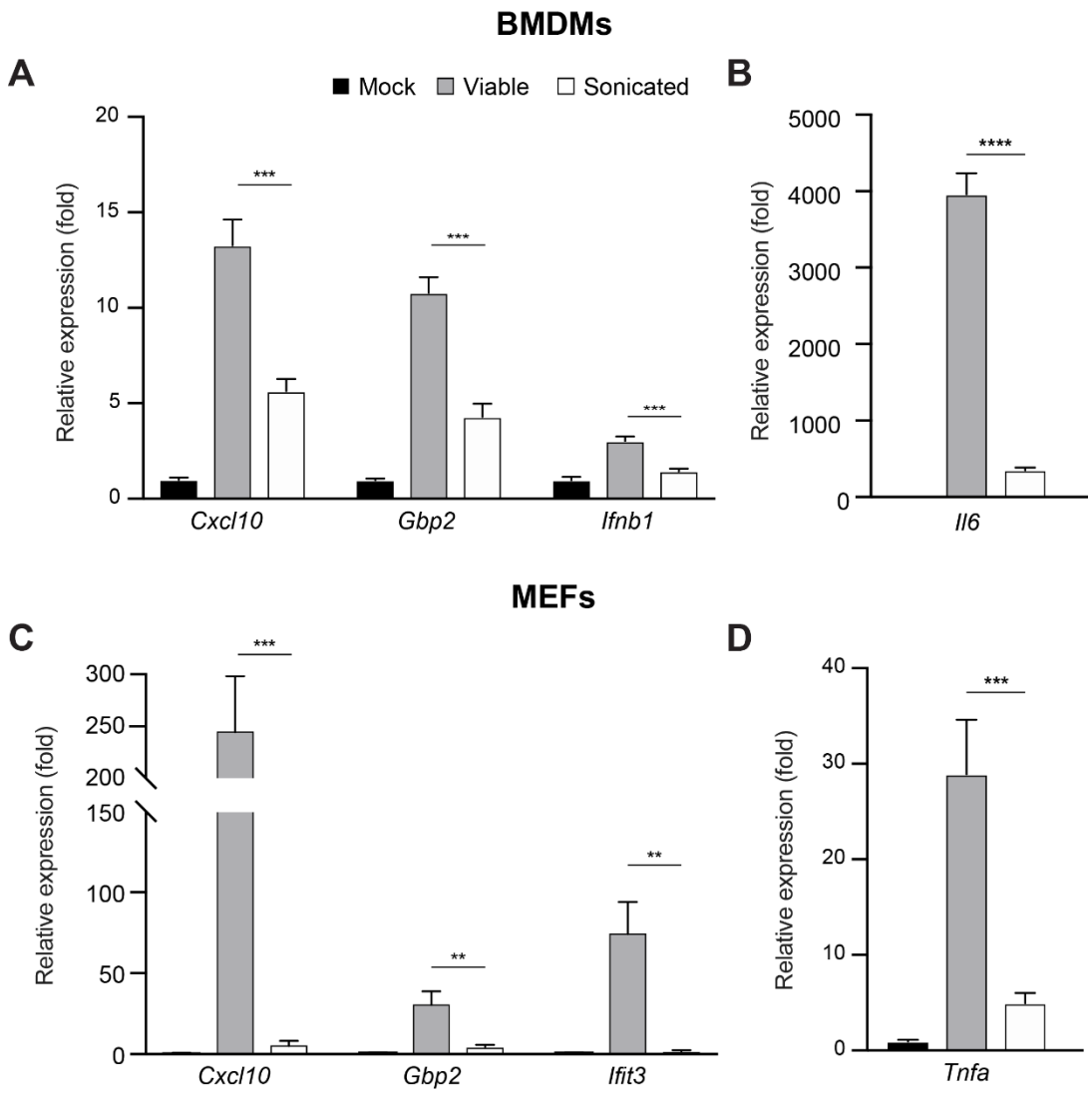

Figure 1 – Viable *B. burgdorferi* induce robust proinflammatory and type I interferon responses in mouse macrophages and fibroblasts. Bone marrow-derived macrophages (BMDMs) or mouse embryonic fibroblasts (MEFs) were co-cultured with viable or sonicated *B. burgdorferi* strain B31-A3 at a MOI of 20 for 6 or 24 hours, respectively, in biologic duplicate. (**A**) qRT-PCR of BMDM interferon-stimulated genes (ISGs) (*Cxcl10* and *Gbp2*) and *Ifnb1* and (**B**) pro-inflammatory cytokine *Il6*. (**C**) qRT-PCR of MEF ISGs (*Cxcl10, Gbp2* and *Ifit3*) and (**D**) inflammatory cytokine *TNFa*. (A) and (B) are averages of biological duplicates from a single experiment (C) and (D) are triplicate biological samples representative of three independent experiments. Error bars represent mean ± SEM. Significance was determined by multiple t tests for all panels. **** $p < 0.0001$, ***$p < 0.001$, ** $p < 0.01$.

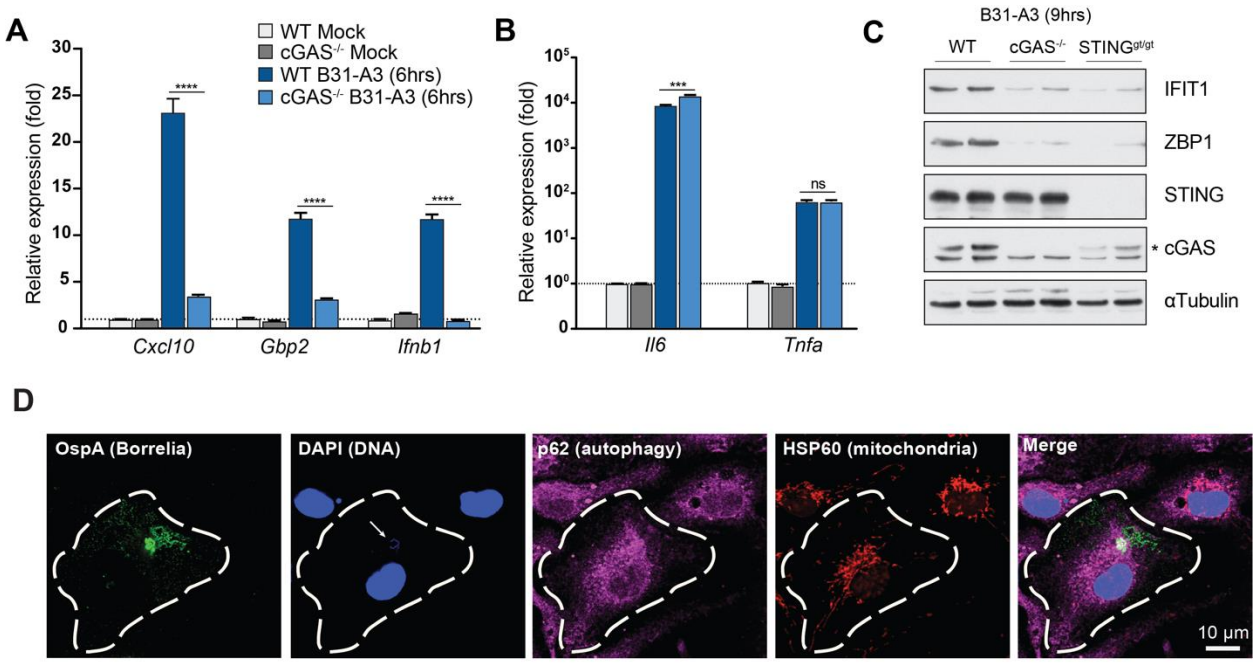

Figure 2 – cGAS governs ISG expression in mouse macrophages exposed to live *B. burgdorferi*. (**A** and **B**) qRT-PCR of ISGs (*Cxcl10, Gbp2*) and *Ifnb1* (A) and inflammatory cytokines (*Il6* and *Tnfa*) (B) in wild-type (WT) and cGAS knockout (cGAS$^{-/-}$) bone marrow-derived macrophages exposed to live *B. burgdorferi* strain B31-A3 for 6 hours at MOI 20 performed in biologic duplicate and technical triplicate. Values are plotted relative to WT mock infected samples. (**C**) Western blots of WT, cGAS$^{-/-}$, and STING deficient (STING$^{gt/gt}$) BMDMs mock infected or exposed to B31-A3 at a MOI 20 for 9 hours. Each lane represents a biological duplicate representative of three independent experiments. (**D**) WT BMDMs were co-cultured with strain B31-A3 at MOI 20 for 3 hours on coverslips. Cells were fixed and stained with antibodies against Borrelial outer surface protein A (OspA), autophagy marker p62, mitochondrial heat shock protein 60 (HSP60), counterstained with DAPI, and subjected to confocal microscopy. Error bars represent mean ± SEM of triplicates. (A) and (B) are representative two independent experiments. One-way ANOVA Tukey post hoc was used in (A) and (B) to determine significance. ****$p < 0.0001$. ns, not significant.

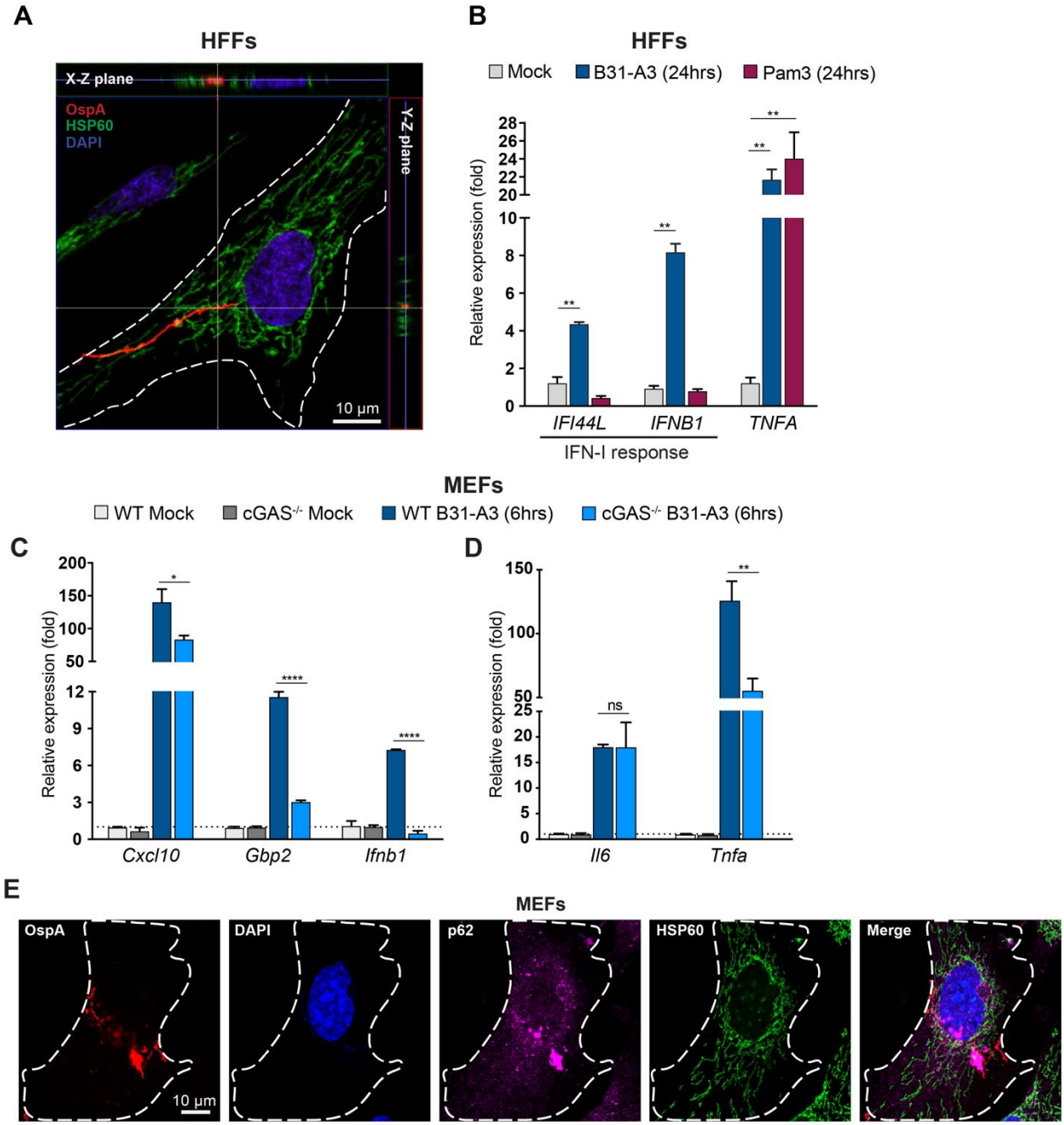

Figure 3 – cGAS governs ISG expression in fibroblasts exposed to live *B. burgdorferi*. (**A** and **B**) Telomerase immortalized human foreskin fibroblasts (HFFs) were co-cultured with *B. burgdorferi* at a MOI of 20. (A) After 3 hours of incubation, cells were fixed and stained with antibodies against Borrelial outer surface protein A (OspA) and mitochondrial heat shock protein 60 (HSP60), counterstained with DAPI, and subjected to confocal microscopy. Z-stack image

reconstitution was performed to localize *B. burgdorferi* and mitochondria. (B) 24 hours after infection, RNA was extracted and qRT-PCR performed to assess ISGs (*IFI44L* and *IFNB1*) and inflammatory cytokine *TNFA*. (**C** and **D**) qRT-PCR of ISGs (*Cxcl10* and *Gbp2*) and *Ifnb1* (C) and inflammatory cytokines (*Il6* and *Tnfa*) (D) in wild-type (WT) and cGAS knockout (cGAS$^{-/-}$) mouse embryonic fibroblasts (MEFs) 6 hours after infection with B31-A3 at MOI 20 performed in biologic duplicate and technical triplicate. (**E**) WT MEFs were co-cultured with strain B31-A3 at MOI 20 for 6 hours on coverslips. Cells were fixed and stained with antibodies against Borrelial outer surface protein A (OspA), autophagy marker p62, mitochondrial heat shock protein 60 (HSP60), counterstained with DAPI, and subjected to confocal microscopy. Error bars represent mean ± SEM of triplicates. Data shown are representative of three independent experiments. One-way ANOVA Tukey post hoc was used in (A), (C) and (D) to determine significance. ****$p < 0.0001$, **$p < 0.01$, *$p < 0.05$, ns, not significant.

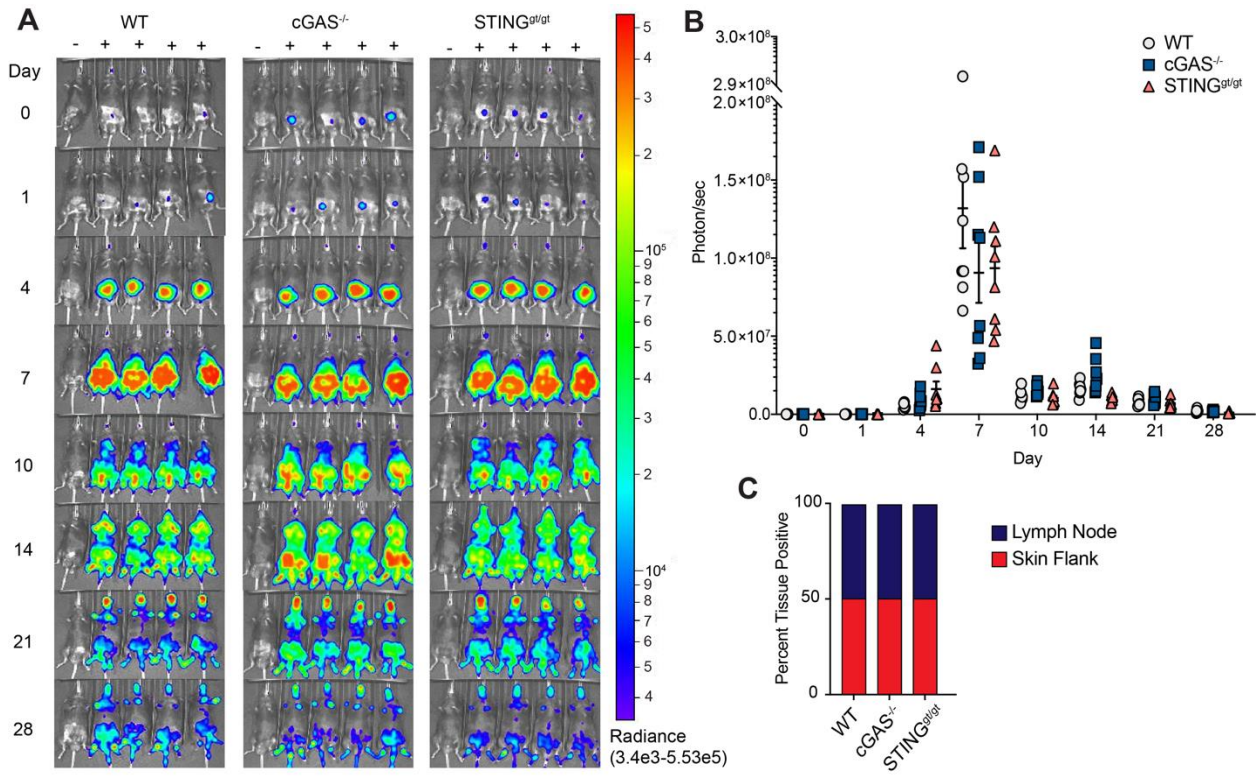

Figure 4 – *B. burgdorferi* infection kinetics and tissue colonization are comparable among WT, cGAS, and STING deficient mice. WT, cGAS$^{-/-}$, and STING$^{gt/gt}$ mice on the C57BL/6J background were infected with 10^5 ML23 pBBE22*luc B. burgdorferi (n = 10/strain, 30 mice total)*. (**A**) Mice were selected randomly and treated with D-luciferin at 1, 4, 7, 10, 14, 21, 28, and 35 days post infection for *in vivo* imaging. For each mouse genotype, the mouse in the first column did not receive D-luciferin to serve as a background control. All images were normalized to the 3.4×10^3 to 5.53×10^5 photons/sec (p/s) and displayed on the same color spectrum scale (right). (**B**) Quantification of bioluminescence in p/s. (**C**) Qualitative assessment of dissemination through tissue outgrowth. At days 28 and 35, 5 mice per strain were sacrificed after completion of imaging. An inguinal lymph node and skin flank were collected for *in vitro* cultivation. Percent of positive cultures is indicated by the y-axis. There was no significant difference in bioluminescence or tissue outgrowth across all mouse genotypes.

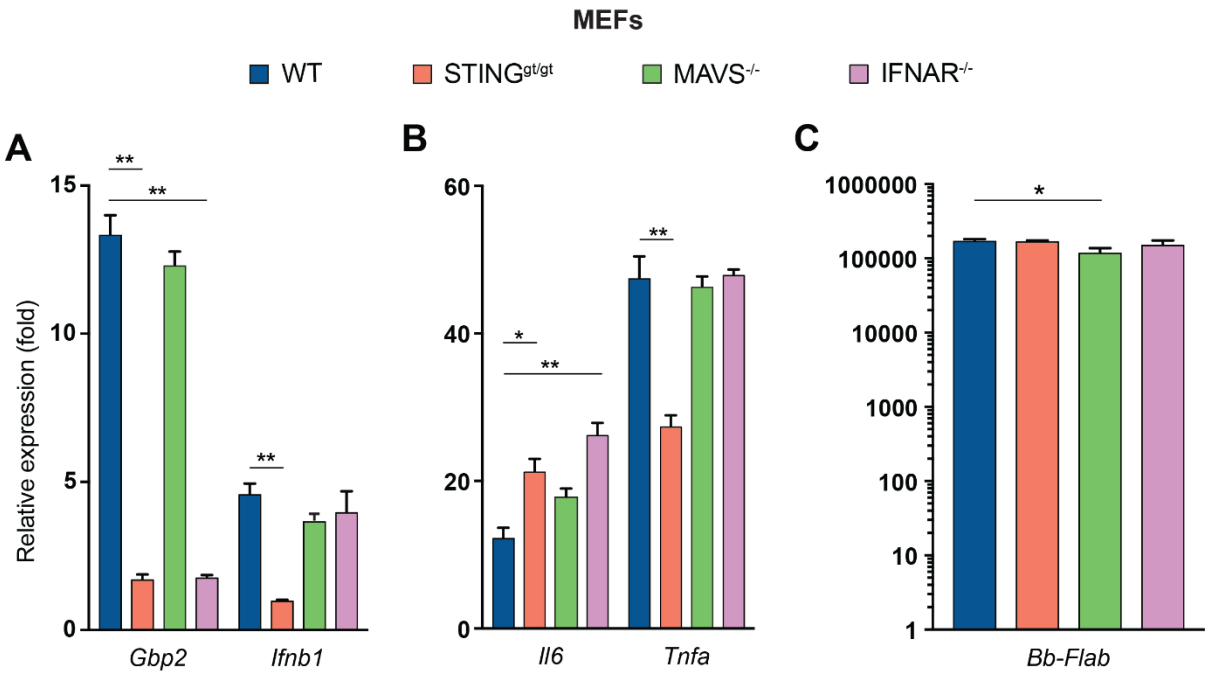

Supplemental Figure 1 – The cGAS-STING-IFNAR signaling axis, but not the MAVS RNA sensing pathway, is responsible for IFN-I responses to *B. burgdorferi*. qRT-PCR of ISG (*Gbp2*) and *Ifnb1* (**A**) and pro-inflammatory cytokines (*Il6* and *Tnfa*) (**B**) in WT, STING deficient (STING$^{gt/gt}$), MAVS knockout (MAVS$^{-/-}$) and IFNAR knockout (IFNAR$^{-/-}$) MEFs after 6 hours of exposure to live *B. burgdorferi* B31-A3 at MOI 20. (**C**) Internalization of *B. burgdorferi* was evaluated in each cell type by qRT-PCR targeting borrelial *flaB.* The experiment was performed in biologic duplicate and technical triplicate. Error bars represent mean ± SEM. One-way ANOVA Tukey post hoc was used to determine significance. $^{**}p < 0.01$, $^{*}p < 0.05$.

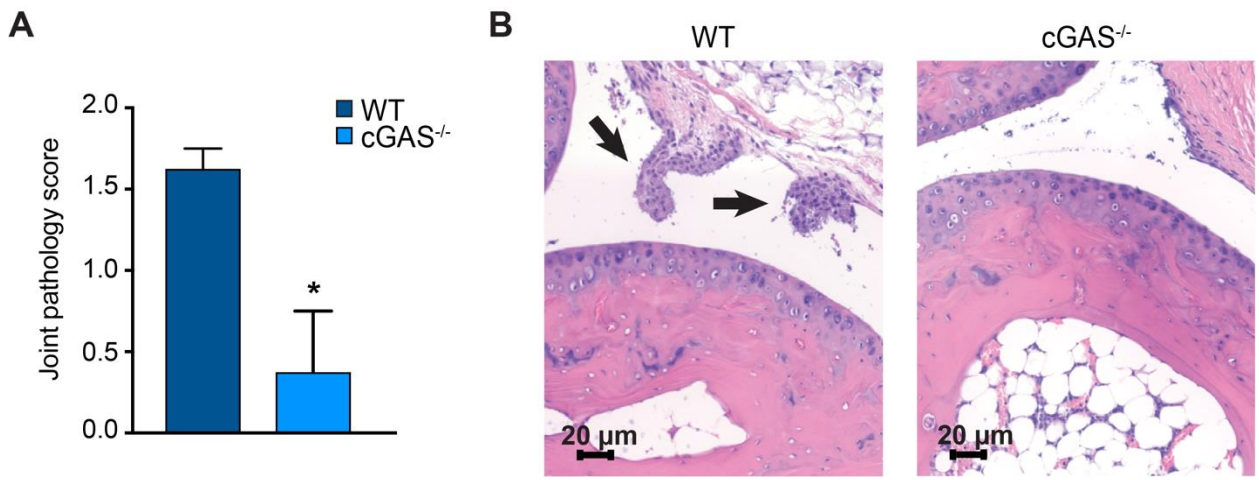

Supplemental Figure 2 – cGAS knockout mice exhibit less joint pathology and inflammation after *B. burgdorferi* infection. WT, cGAS$^{-/-}$, and C57BL/6 mice were infected with 10^5 ML23 pBBE22*luc B. burgdorferi (n = 10/strain, 30 mice total)*. Joint tissue was collected from 5 mice per genotype at 28 days post infection. (**A**) Average overall lesion score with error bars showing mean ± SEM. (**B**) Rear ankles were fixed and hematoxylin and eosin stained. Images were obtained using 200X magnification. Arrows indicate areas of synovial papillary hyperplasia. Significance was determined by student's t test. *$p < 0.05$.